can obtain pulses '0', '0', '0', '0', '1', '0', '0', '0', '0', and '0' (pattern I) when not using the delay and pulses '0', '0', '0', '0', '1', '1', '0', '0', '0', and '0' (pattern II) when using the delay. The two patterns correspond to the 100Gbit/s OTDM signal. The pulsewidth of the OTDM signal is then broadened by using an optical fibre with a total chromatic dispersion of –60ps/nm. An 80km dispersion-shifted fibre (DSF with a zero dispersion wavelength of 1552nm) was used as the transmission fibre and the optical signal waveforms were measured before transmission (X) and after transmission (Y) with an optical sampling system [4]. Fig. 3*a* and *b* are the measured optical signal waveforms. The upper and lower Figures show the pattern I signal and pattern II signal, respectively.

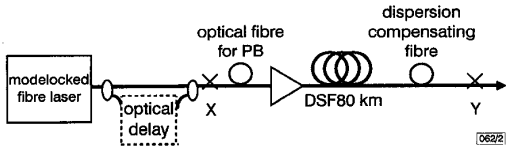

Fig. 2 *Experimental setup*

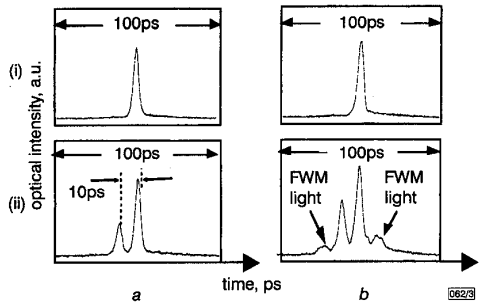

Fig. 3 *Pulse shape*

(i) Pattern I
(ii) Pattern II
a Before transmission (at point X of Fig. 2)
b After transmission (at point Y of Fig. 2)

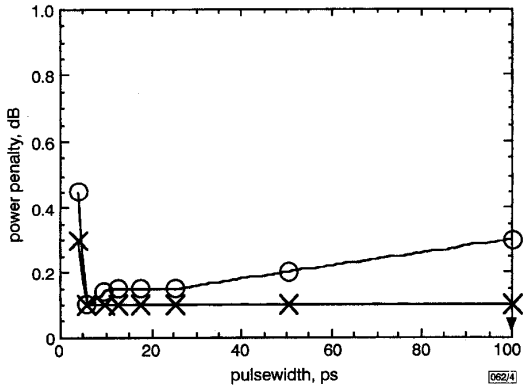

Fig. 4 *Pulsewidth dependence of power penalty*

100Gbit/s, pulsewidth before PB = 4ps, average power = +10dBm, signal wavelength = 1553nm, zero dispersion wavelength = 1552nm
O SPM and inter-bit FWM (pattern II)
× SPM (pattern I)

From these results, it is clear that inter-bit FWM occurred only in the pattern II signal. We also numerically examined the influence of the single-pulse SPM-GVD effect and inter-bit FWM effect. In the simulation, we assumed that the optical signal had a repetition rate of 100Gbit/s, a pulsewidth of 4ps, an average input power of +10dBm, and a wavelength of 1553nm. The length and zero-dispersion wavelength of the transmission fibre were set at 80km and 1552nm, respectively. Fig. 4 depicts the relationship between the pulsewidth of the optical pulses and the power penalty caused by single-pulse SPM-GVD or inter-bit FWM. The power penalty is estimated using channel crosstalk. The channel crosstalk is defined as the ratio of the optical energy loss to the original signal energy in a time slot. The influence of SPM-GVD can be suppressed by broadening the pulse. In contrast, the influence of inter-bit FWM increases with the broadening of the pulsewidth. This is because the larger the pulsewidth becomes, the more the frequency components interact. This feature intensifies when the broadened pulsewidth is over the time slot. Therefore, there is an optimum pulsewidth; in the 100Gbit/s case, this is 6ps. This result indicates that pulse broadening is most effective when the pre-broadened pulsewidth is adjusted to this optimum value.

Conclusion: We showed that pulse broadening over the time slot causes inter-bit FWM, which degrades the OTDM transmission characteristics. We have also confirmed this effect experimentally by measuring OTDM signal waveforms, and have numerically estimated the magnitude of the effect. Adjusting the pulsewidth (to 6ps in the case of the 100Gbit/s case) is the best way to reduce the nonlinear effect in an optical fibre.

Acknowledgment: We would like to thank I. Kobayashi for his encouragement, and A. Takada for fruitful discussions.

16 June 1998
Elecronics Letters Online No: 19981110

I. Shake, H. Takara, K. Mori, S. Kawanishi and Y. Yamabayashi (*NTT Optical Network Systems Laboratories, 1-1 Hikari-no-oka, Yokosuka, Kanagawa 239-0847, Japan*)

References

1 MIYAMOTO, Y., KATAOKA, T., SANO, A., HAGIMOTO, K., AIDA, K., and KOBAYASHI, Y.: '10Gbit/s, 280km nonrepeatered transmission with suppression of modulation instability', *Electron. Lett.*, 1994, **10**, pp. 797–798

2 KAWANISHI, S., TAKARA, H., MORIOKA, T., KAMATANI, O., and SARUWATARI, M.: '200Gbit/s 100km time-division-multiplexed optical transmission using supercontinuum pulses with prescaled PLL timing extraction and all-optical demultiplexing', *Electron. Lett.*, 1995, **10**, pp. 816–817

3 KAWANISHI, S., TAKARA, H., MORIOKA, T., KAMATANI, O., TAKIGUCHI, K., KITOH, T., and SARUWATARI, M.: 'Single channel 400Gbit/s time-division-multiplexed transmission of 0.98 ps pulses over 40km employing dispersion slope compensation', *Electron. Lett.*, 1996, **10**, pp. 916–918

4 TAKARA, H., KAWANISHI, S., YOKOO, A., TOMARU, S., KITOH, T., and SARUWATARI, M.: '100Gbit/s optical signal eye-diagram measurement with optical sampling using organic nonlinear optical crystal', *Electron. Lett.*, 1996, **24**, pp. 2256–2258

Multichannel add/drop and cross-connect using fibre Bragg gratings and optical switches

Shien-Kuei Liaw, Keang-Po Ho and Sien Chi

A dynamically selective wavelength add/drop multiplexer (WADM) and a multiwavelength cross-connect (M-XC) configuration for dense wavelength division multiplexed networks are proposed. Multiple channels add/drop and/or cross-connect can be realised according to the control of the optical switches and fibre Bragg gratings arrangement. The selective WADM and M-XC devices could provide more reconfigurable flexibility and survivability in WDM networks.

Introduction: Recently, significant research efforts have been devoted to the design of high-capacity, flexible, reliable and transparent multiwavelength optical networks [1, 2]. Wavelength add/drop multiplexer (WADM) and multiwavelength cross-connect (M-XC) switches will play key roles in future optical dense wavelength division multiplexing (WDM) networks. The WADM is used for selectively dropping and inserting optical signals into the WDM network. It can reduce the processing load and latency in intermediate nodes by handling through-traffic. The closed related M-XC is configurable on a link-by-link basis to allow optimisation of capacity allocation, management, and scalability of network size, especially in a reconfigurable ring topology.

Conventional optical WADMs usually consist of a $1 \times N$ demultiplexer (DMUX) followed by an $N \times 1$ multiplexer (MUX). A certain channel is dropped and/or added at each WADM unit according to a specific add-drop plan [3]. A wavelength selective (i.e. rearrangable) M-XC can be implemented by adding a space division switch in between a WDM MUX/DMUX pair to select wavelengths and rearrange them in the spatial domain. This approach seems not to be very practical because the cost and noise associated with the optoelectronic repeater stages will make it difficult to construct a suitable electronic switch [4]. Recently, two system experiments for one-channel selective add-drop [5] and two-channel cross-connect [6] from trunk lines carrying several signals, by integrating some reflective fibre Bragg gratings (FBGs) with optical switches (OSWs), were demonstrated. Though another WADM configuration based on FBGs and OSWs for simultaneous multiple wavelength add/drop via an FBG chain was also proposed [7], it seems less practical since the inclusion of multiple gratings would require an extra DMUX in the drop port and an extra MUX in the add port. In this Letter, we propose a WADM and M-XC configuration for simultaneous multiple wavelengths add-drop and cross-connect, respectively, by using FBGs, optical circulators (OCs) and OSWs.

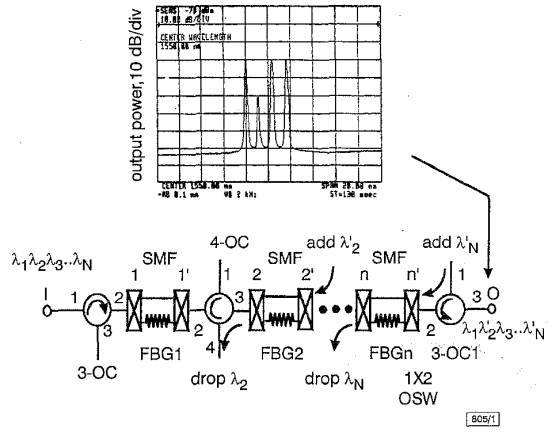

Fig. 1 *Schematic diagram of proposed WADM configuration using optical circulators, optical switches and fibre Bragg gratings*

Inset: pass-through (one-wavelength dropped) spectrum for WADM at output port O
OC: optical circulator, OSW: optical switch, FBG: fibre Bragg grating

Proposed configurations for WADM and M-XC: Fig. 1 shows a schematic diagram of the proposed wavelength-selective WADM device. One pair of a three-port OC and a 1×2 OSW are located at both the input and the output ports with n ADM units cascading in sequence between them. Each ADM unit consists of one piece of FBG_i with the central reflective wavelength matching the WDM signal λ_i (i = 1, 2, 3, ..., N), one piece of singlemode fibre (SMF), an 1×2 OSW and a three/four-port OC. The optical signals are launched into the first three-port OC at the left-hand side. Some of these OSW-pairs are switched to the FBG port(s) rather than the SMF port(s) for dropping and re-adding optical signal(s) with corresponding wavelength(s). For example, signal i drops or passes through the cascading FBG chains depending on whether the corresponding 1×2 OSW pair is switched to FBG_i or SMF. When λ_i drops from port three/four of the three/four-port OC, a new signal wavelength λ'_i with the same central wavelength as λ_i will add from port one of the four/three-port OC to the fibre link after it is reflected by FBG_i. Other optical signals not dropped by the FBG chains will pass through all the ADM units and then continue their forward propagation.

Fig. 2 shows the proposed configuration of the selective M-XC. N cross-connect units, each consisting of one piece of FBG_i (i = 1, 2, 3, ..., N) matching the WDM channel signal i, a piece of SMF and a 2×2 OSW, are cascaded one by one and inserted in between the three-port OC and the 1×2 OSW pair. For example, by simultaneously switching some of these switch-pairs to the desired FBG ports such as FBG_2 and FBG_4, λ_2 and λ_4 of the upper fibre link will reflect and leave from port 3 of the OC1, continuing their forward propagation (termed here as passed-through) in the same fibre link. The channel signals other than λ_2 and λ_4 are spatially cross-connected (here, passed through the N cross-connect units) to the lower fibre link. Meanwhile, channel signals other than λ'_2 and λ'_4 of the lower fibre link are cross-connected to the upper fibre link. Thus, multiple channel cross-connection can be realised. There are two input ports (I1 and I2) as well as two output ports (O1 and O2) in the M-XC configurations. These two input ports can operate in the same direction or in opposite directions (i.e. bidirectional) by simply re-arranging the lower three-port (number 1, 2 and 3) OC in the clockwise or anti-clockwise direction, dependent on the network structures in which the M-XC is located. The power loss for both WADM and M-XC configurations due to the cascading of fibre components and devices can be compensated easily by using optical amplifiers.

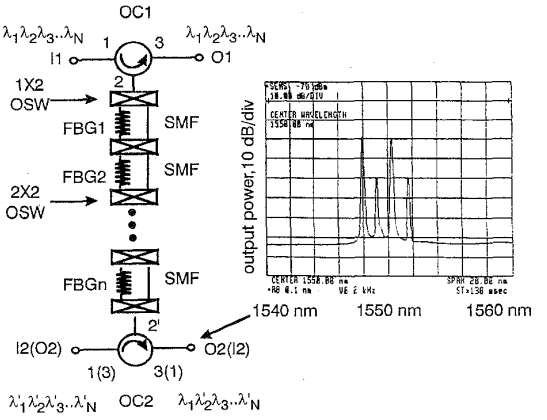

Fig. 2 *Proposed dynamically selective multiwavelength cross-connect configuration*

Inset: two-wavelength cross-connect spectrum for M-XC at output port O2

Experimental results of optical spectra: To investigate the feasibility of these proposed FBG and OSW-based WADM and M-XC, one set of four WDM channel signals (λ_1, λ_2, λ_3 and λ_4) with 1.3nm channel spacing in the 1.55μm band are launched from port I of Fig. 1 and port II of Fig. 2 to demonstrate the one-wavelength drop (without re-add) and two-wavelength cross-connect functions, respectively. The inset of Fig. 1 shows the resulting output spectrum at point O of the pass-through signals for the WADM, and the inset of Fig. 2 shows the resulting output spectrum at point O2 of the cross-connect signals for the M-XC. The interport insertion loss of the OCs is 1.2dB and the insertion loss is 0.5dB for each OSW from the common port to any other ports, respectively. The isolation of each OC is > 48dB. The 3dB bandwidth and reflectivity of the FBGs used in these two experiments are 0.25nm and 99%, respectively. In Fig. 1, one small spectral component contaminating the other three passed-through signals with −20dB crosstalk level results from the 1% transmittivity of FBG_2. A similar result can also be found in Fig. 2. Further reduction in the crosstalk level for upgrading system performance is possible by improving the FBG reflectivity.

Conclusion: In summary, two configurations are proposed for multiple wavelengths add-drop and cross-connect based on FBGs and OSWs. The WADM and M-XC devices have potentially large add-drop efficiency, low channel crosstalk, uniform channel loss, high scalability and low cost, and hence may provide increased flexibility and survivability in WDM networks.

Acknowledgments: We would like to thank Y.-K. Tu and J.-W. Liaw of the Chung-Hwa Telecommunication Laboratories in Taiwan for helpful suggestions. The work was supported in part by Grant No. NSC-087-2215-E-009-012 of the National Science Council in Taiwan, R.O.C.

15 June 1998
Electronics Letters Online No: 19981098

Shien-Kuei Liaw and Sien Chi (*Institute of Electro-Optical Engineering, National Chiao-Tung University, 1001 Ta Hsueh Road, Hsin-Chu 300, Taiwan, Republic of China*)

E-mail: u8424802@cc.nctu.edu.tw

Keang-Po Ho (*Department of Information Engineering, The Chinese University of Hong Kong, Shatin, New Territory, Hong Kong*)

References

1 FUJIWARA, M., GOODMAN, M.S., O'MAHONY, M.J., TONGUZ, O.K., and WILLNAR, A.E.: 'Special Issue on multi-wavelength optical technology and networks', *J. Lightwave Technol.*, 1996, **14**, pp. 932–935

2 ELREFAIE, A.F., GOLDSTEIN, E.L., ZAIDI, S., and JACKMAN, N.: 'Fiber amplifier cascades with gain equalization in multi-wavelength unidirectional inter-office ring networks', *IEEE Photonics Technol. Lett.*, 1993, **5**, pp. 1026–1028

3 ANTONIADES, N., ROUDAS, I., WANGER, R.C., and HABIBY, S.F.: 'Simulation of ASE noise accumulation in a wavelength add/drop multiplexer cascade', *IEEE Photonics Technol. Lett.*, 1997, **9**, pp. 1274–1276

4 SHARMA, R., and MACDONALD, R.I.: 'A signal transparent 10 × 10 space-division optoelectronic switch core for virtual-transparent path-based multiwavelength networks', *IEEE Photonics Technol. Lett.*, 1997, **15**, pp. 1522–1529

5 LIAW, S.-K., CHEN, Y.-K., and LEE, C.-C.: 'System demonstration of wavelength tunable multiple-ITU-WDM-channel add/drop multiplexer using an optical-switch pair and fiber Bragg gratings'. OFC'98, San Jose, CA, 1998, Paper WM39

6 CHEN, Y.-K., LIAW, S.-K., and LEE, C.-C.: 'Multiwavelength dynamically selective cross connect based on fiber Bragg gratings and optical switches'. CLEO'98, San Jose, CA, 1998, Paper CWT4

7 OKAYAMA, H., OZEKI, Y., KAMIJOH, T., XU, C.Q., and ASABAYASHI, I.: 'Dynamic wavelength selective add/drop node comprising fibre gratings and optical switches', *Electron. Lett.*, 1997, **33**, pp. 403–404

Thermal decay of gratings written in hydrogen-loaded germanosilicate fibres

I. Riant and B. Poumellec

A new description of the thermal decay of gratings written in hydrogen-loaded germanosilicate fibres is proposed. This model allows an accurate prediction of lifetime.

The thermal stability of germanosilicate fibre Bragg gratings has now been heavily studied [1 – 5]. A model has been proposed [1] to describe thermal decay and to predict the lifetime of germanosilicate fibre Bragg gratings, leading to very good fits in the case of unloaded fibres [1, 2]. The model assumes that thermal decay follows a law of the type $1/(1+At^{\alpha})$, where t is the time and A and α are two fitting constants. The mechanisms underlying this model postulate that carriers excited during writing are then trapped in a broad distribution of trap states and that the rate of thermal depopulation is a function of the trap depth. However, several authors [2 – 5] have found that this model does not completely apply to hydrogen (H_2)-loaded fibres. Robert *et al.* [4] needed to use two distributions to account for short and long term decays, and Baker *et al.* [2] proposed a log-time based model to fit decay characterics and predict lifetime. Kannan *et al.* [3] also observed a divergence in the case of H_2-loaded fibres, and they suggest building an empirical curve by plotting all the normalised index modulations Δn_{mod} for the different temperatures according to the variable $k_B T\ln(\nu t)$, in which k_B is the Boltzman constant, T is the temperature, t is the time and ν is a constant that allows them to predict long term behaviour.

Following the description of [2] and the approach of [3], we have plotted the normalised Δn_{mod} against $k_B T\ln(t)$, shown in Fig. 1. The gratings were written using an excimer laser emitting at 248nm with a fluence of ~ 200mJ/cm² at 10Hz. The grating length was 500μm. The photoinduced index modulation was 2×10^{-3}; the studied temperatures were 175, 200, 250, 300, 350, 400 and 500°C, and three gratings were heated at each temperature. Based on the results from the authors mentioned, we expected the curves to be linear and shifted by a quantity equal to $k_B T\ln(\nu)$. Indeed, our curves are linear. Baker *et al.* [2] also noticed that at 85°C, there was no decay for a while. This could not be confirmed here since we did not perform any measurements at such low temperatures. A linear fit of these curves leads to a unique slope which is temperature independent. This slope is equal to $-0.37 \pm 0.05\text{eV}^{-1}$ (see Fig. 2). The origin ordinate, on the contrary, varies linearly with temperature. This could be expected since it contains a term proportional to $k_B T\ln(\nu)$. A linear fit yields $-(9.7 \pm 0.5 \times 10^{-4}\text{ in K}^{-1}) \times (T\text{ in }K) + 1.34 \pm 0.03$ (Fig. 2).

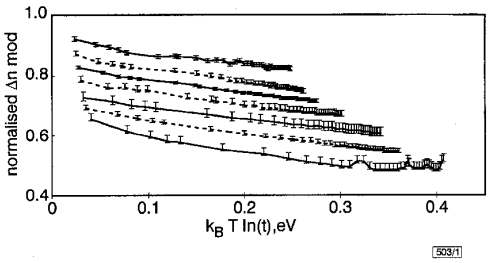

Fig. 1 *Normalised index modulation against quantity $k_B T\ln(t)$*

k_B: Boltzman constant, T: temperature in K, t: time in minutes. Each curve corresponds to a different temperature; from top to bottom: 175, 200, 250, 300, 350, 400 and 500°C. Three gratings were heated for each temperature, but only one decay was reported for simplicity. Error bars added to represent decay of the two other gratings for each temperature

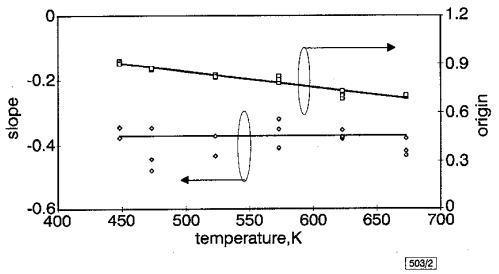

Fig. 2 *Slopes and origin ordinates against temperature for curves of Fig. 1*

Three gratings for each temperature taken into account

To further elucidate the interpretation of the coefficients and to determine the long term stability, it is necessary to use a correct distribution function associated with these results. In an attempt to find this distribution, we used the VAREPA model [6]. According to this model, a change of index during erasure occurs after a monomolecular reaction ($A \leftarrow B$) with a rate constant k. The expression for k is $k = k^0 \exp(-E/k_B T)$, with k^0 as the pre-exponential factor and E as the erasure activation energy. B is assumed to be the species responsible for the index change and A is the precursor. We use the idea of demarcation energy E_d, below which the physico-chemical reaction corresponding to erasure is carried out. The remaining content of B after a time t and at a temperature T, assuming a saturated grating, is then given by

$$[B](t) = A_0 \int_{E_d}^{\infty} g(E)\, dE \qquad (1)$$

where A_0 is a constant and g is the distribution function for erasure. The expression of the demarcation energy is $E_d = k_B T\ln(k^0 t)$ [6]. After analysing the data, it appears that the distribution function must be a normalised constant distribution limited by E_{min} and E_{max}:

$$g(E) = \begin{cases} 0 & E < E_{min} \\ \frac{1}{E_{max} - E_{min}} & E_{min} < E < E_{max} \\ 0 & E_{max} < E \end{cases} \qquad (2)$$

(i) When $E_d < E_{min}$ the decay has not yet begun. This is the part observed by [2] at 85°C when the grating strength remained constant for a while. By replacing eqn. 2 in eqn. 1, we obtain $[B](t) = A_0$. The erasure does not begin until a time corresponding to the time for E to reach E_{min}.